Journal of Thermal Analysis, Vol. 50 (1997) 125-135

Dedicated to Prof. Menachem Steinberg on the occasion of his 65th birthday

NONCONVENTIONAL METHODS FOR OBTAINING HEXAFERRITES
I. Lead hexaferrite

Oana Carp[a], *E. Segal*[b], *Maria Brezeanu*[c], *Ruxandra Barjega*[d] *and N. Stanica*[a]

[a]Institute of Physical Chemistry, Splaiul Independentei, Nr. 202, sector 6, Bucharest
[b]Department of Physical Chemistry, Faculty of Chemistry, University of Bucharest, Bulevardul Republicii Nr. 13, Bucharest
[c]Department of Inorganic Chemistry, Faculty of Chemistry, University of Bucharest, Dumbrava Rosie Street, Nr. 23, sector 2 Bucharest
[d]ZECASIN S. A., Chemical Research & Development & Production, Splaiul Independentei Nr. 202, sector 6, Bucharest, Romania

Abstract

Small particles of $PbFe_{12}O_{19}$ have been synthesized. X-ray diffraction, thermal analysis and magnetic investigations have been conducted in order to obtain information on the mechanism of lead hexaferrite formation.

Keywords: lead hexaferrite, nonconventional methods, precursors

Introduction

The ferrites of magnetoplumbite type with the general formula $MFe_{12}O_{19}$ (M=Ba, Sr, Pb) are hard ferrites used as permanent magnets.

In order to obtain hexaferrites with high performance parameters, methods of synthesis which lead directly to small particles, thus eliminating grinding procedures are necessary. Breaking and grinding introduce strains in the crystalline lattice which change the magnetic properties in an uncontrolled manner [1–3]. Among the synthesis procedures used to obtain such oxide systems coprecipitation [3–7], crystallization [8–10], sol-gel techniques [11–16], hydrothermal techniques [17–18], decomposition of organometallic compounds [19], and liquid mixt techniques [21–22] are to be mentioned.

This work, the first from a series dedicated to the synthesis of hexgonal ferrites using unconventional methods aims a generalization of some procedures applied to spinellic ferrites in order to obtain hexaferrites [22–26].

0368–4466/97/ $ 5.00

John Wiley & Sons Limited
Chichester

Experimental

Lead nitrate $Pb(NO_3)_2$ and iron oxalate $FeC_2O_4 \cdot 2H_2O$, reagent grade, supplied commercially (Romanian production – Reactivul) were used as raw materials. A suspensions of the two compounds with a stoichiometric ratio $FeC_2O_4 \cdot 2H_2O/Pb(NO_3)_2$=12 in hot water is brought to $pH \sim 13$ by adding NaOH solution (25% *w/w*). The reaction mixture is kept under stirring with or without boiling for periods changing from 5 min to 20 h. The precipitate obtained by hydrolytic decomposition of the raw materials is then filtered off and washed with water.

Three forms of the synthesized precursors were further investigated: P_1 (time of mixing 5 min, with boiling), P_2 (time of mixing 10 h, at room temperature) and P_3 (time of mixing 20 h, with boiling).

In order to characterize the precursors as well as their calcination products, IR spectrometry, X-ray diffraction, thermal analysis and magnetic measurements were applied.

The IR spectra were recorded with a SPECORD M–80 ZEISS JENA spectrophotometer, in the range 400–4000 cm^{-1} using the KBr pellet technique.

The X-ray diffractograms were recorded with a DRON 3 X-ray diffractometer with CoK_α radiation.

The heating curves (TG-DTG-DTA) were obtained by using a Paulik-Paulik-Erdey type Q-1500 derivatograph, in static air atmosphere, at various heating rates. 100 mg samples were used. In order to record the DTA curves, α-alumina was used as an inert material.

The magnetic properties (the saturation magnetization) at room temperature were determined by means of the permeameter method.

Results and discussion

Precursors

X-ray diffraction data pointed to the presence of a mixture consisting of two crystalline phases, magnetite and lead carbonate hydroxide, hydrocerussite (Table 1). These crystalline phases are characterized by broad diffraction lines indicating small particles. The mean crystallite sizes calculated by the Sherrer formula [28] from the most intense four diffraction lines are listed in Table 2.

The same phases have been identified in the IR – spectra (Fig. 1) exhibiting a band characteristic of the bending modes of water and OH^{-1} group [28] (at 1600 cm^{-1}), the bands corresponding to the vibration modes of the carbonate anion slightly shifted with respect to the same anion in Na_2CO_3 (900, 1050 and 1400 cm^{-1}) and the band characteristic of the Fe–O bonds [29] (at 450 and 600 cm^{-1}) corresponding to iron located in octahedral and tetrahedral positions, respectively.

Table 1 X-ray diffraction data for the precursors of lead hexaferrite

Magnetite ASTM 19–629			P_1/5 min		P_2/10 h		P_3/20 h		$Pb_3(CO_3)_2(OH)_2$ ASTM 13–131			P_1/5 min		P_2/10 h		P_3/20 h	
hkl	d_{hkl}	I/I_o	d_{hkl}	I/I_o	d_{hkl}	I/I_o	d_{hkl}	I/I_o	*hkl*	d_{hkl}	I/I_o	d_{hkl}	I/I_o	d_{hkl}	I/I_o	d_{hkl}	I/I_o
111	4.85	8	–	–	–	–	–	–	003	7.80	5	–	–	–	–	–	–
220	2.967	20	2.97	38	3.00	41	3.00	44	101	4.47	60	4.46	41	4.50	62	–	–
311	2.532	100	2.53	100	2.55	100	2.56	100	012	4.25	60	4.25	50	4.28	43	3.68	80
222	2.424	8	–	–	–	–	–	–	104	3.61	90	3.61	84	3.63	71	3.33	92
400	2.009	20	2.10	41	2.10	33	2.12	29	015	3.09	90	3.29	100	3.30	95	–	–
422	1.715	10	1.71	21	1.72	15	1.72	13	107	2.71	20	2.72	24	–	–	–	–
511	1.616	30	1.62	28	1.62	27	1.62	29	110	2.62	100	2.63	76	2.64	100	2.66	100
									009								
440	1.485	40	1.48	48	1.48	33	1.49	49	018	2.61	30	–	–	–	–	–	–
									021	2.49	10	–	–	–	–	–	–
									202	2.23	50	2.23	65	–	–	–	–
									024	2.12	30		27	–	–	–	–

The presence of magnetite was also confirmed by the ferromagnetism exhibited by the three investigated precursors.

Considering the experimental conditions of the synthesis of the precursors, the following statements can be made:

– the two crystalline phases are Fe_3O_4 and $Pb_3(CO_3)_2(OH)_2$ and they are formed even after a short mixing (5 min);

– on increasing the time of mixing, the amount of crystalline Fe_3O_4 increases and the amount of hydroxocarbonate decreases. This statement is supported qualitatively by: a decrease in the intensities corresponding to the IR bands of the carbonate anion with the time of mixing and the existence of only the most intense diffraction lines of hydroxocarbonate in the X-ray diffractogram recorded after 20 h of mixing. Qualitatively the same statement is supported by the ratio of the most intense diffraction lines $I_{311}Fe_3O_4/I_{009}Pb_3(CO_3)_2$ (Table 2) and the values of the saturation magnetization which both increase with the time of mixing.

Table 2 Properties of the precursors

Precursor	P_1/5 min	P_2/10 h	P_3/20 h
Mean crystallite size			
Fe_3O_4 (Å)	210	215	245
$Pb_3(CO_3)_2(OH)_2$ (Å)	336	262	210
Lattice parameters			
Fe_3O_4 (Å)*	a_0= 8.386	a_0= 8.434	a_0= 8.462
$Pb_3(CO_3)_2(OH)_2$ (Å)**	a_0= 5.24	a_0= 5.30	a_0= 5.37
	c_0=23.82	c_0=23.70	c_0=23.87
$V Fe_3O_4/V_{ASTM} Fe_3O_4$	0.996	1.014	1.024
$V Pb_3(CO)_2(OH)_2/$			
$V_{ASTM}Pb_3(CO)_2(OH)_2$	1.003	1.021	1.024
$I_{311}Fe_3O_4/I_{009}Pb_3(CO)_2(OH)_2$	1.078	2.400	4.556
σs(uem/g)	24.37	34.36	54.38

*a_0(ASTM 19–629)=8.396

**a_0(ASTM 13–131)=5.24; c_0(ASTM 13–131)=23.74

The mean crystallite sizes of magnetite remain practically constant with the mixing time while decrease is recorded for the lead hydroxocarbonate. Probably the latter phenomenon is due to the destruction of the compound during the reaction.

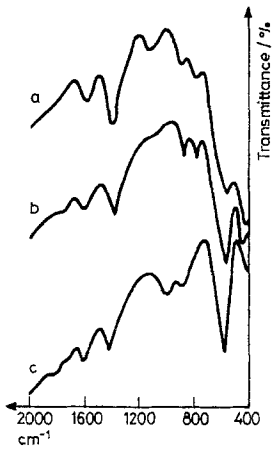

Fig. 1 IR spectra of precursor P_1(a), precursor P_2(b) and precursor P_3(c)

Thermal analysis

The derivatograms (Fig. 2) and the data listed in Table 3 show that: – the decomposition of the precursors obtained after 5 min and 10 h of mixing (P_1 and P_2) occur in three steps corresponding to the release of humidity, absorbed water and to the decomposition of the lead hydroxocarbonate. The thermal behavior of the precursor P_3 obtained after 20 h of boiling and mixing is different in comparison with the other two precursors. The first step corresponding to the release of humidity (0.77%) is followed by an increase in mass corresponding to the oxidation of Fe_3O_4 to γ-Fe_2O_3 (0.88%). This change of magnetite confirmed by the

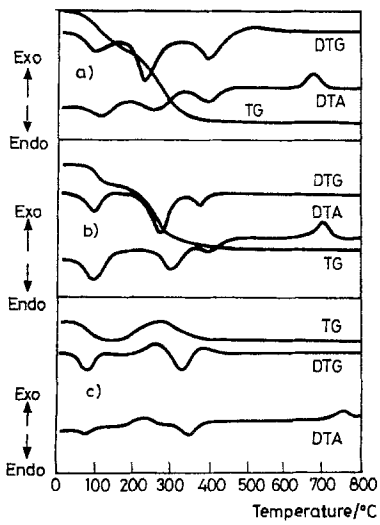

Fig. 2 Simultaneous TG/DTG/DTA curves. a – precursor P_1, b – precursor P_2, c – precursor P_3

Table 3 Thermal analysis of the investigated precursors

Precursor	T_i–T_f	Mass loss/ %	The thermal effect	Assignation
P_1/5 min	60–140	2.15	endo	release of humidity
	140–300	5.27	endo	release of absorbed water
	300–410	1.15	endo	decomposition of hydroxocarbonate
	685**	phase change	exo	ferritization or crystallization of hexaferrite
P_2/10 h	75–130	1.48	endo	release of humidity
	130–305	2.97	endo	release of absorbed water
	305–421	0.89	endo	decomposition of hydroxocarbonate
	703**	phase change	exo	ferritization or crystallization of hexaferrite
P_3/20 h	50–96	0.77	endo	release of humidity
	186–278	0.88***	endo	oxidation of Fe_3O_4 to γ-Fe_2O_3
	278–375	0.94	endo	decomposition of hydroxocarbonate
	762**	phase change	exo	ferritization or crystallization of hexaferrite

*T_i-initial temperature of thermal transformation
T_f-final temperature of thermal transformation
**maximum temperature of DTA peak
***mass gain

IR spectra as well as by X-ray analysis detected only for this precursor, is due to a certain overlap between the release of absorbed water and the oxidation of Fe_3O_4. The slight mass decrease (0.94%) which has been evidenced in the temperature range 240–400°C could be assigned to traces of hydroxocarbonate from the precursor. The final decomposition temperatures for all the three precursors are relatively low (400°C).

An exothermic peak in the range 670–700°C for P_1 and P_2 and 750–775°C for P_3 which can be associated with the ferritization or to the crystallization of the hexaferrite was observed. The activation energy associated with this change was evaluated using Kissinger's method [30], from the variation of the peak temperature T_{max} with the heating rate.

Using four heating rates (1.7, 4.8, 7.8 and 10.5 K min^{-1}) the following values were obtained for the activation energy:

P_1–347.7 kJ mol^{-1}
P_2–333.6 kJ mol^{-1}

For the compound P_3 we could not evaluate accurately the activation energy of the phase change, due to the difficulties in determining the T_{max} value as the corresponding exothermic effect on the DTA curve is very small.

Oxide products

The phase compositions of the calcination residues were found by using X-ray diffraction and magnetic data. For the evidenced phases, changes in the composition with time were evaluated by the ratio of the average main XRD intensities (higher than 10 relative intensity). The mean size of crystallites was evaluated using the Sherrer formula for the same peaks. The temperatures of the thermal treatments were chosen before and after the phase transformation.

Before commenting the results, it has to be mentioned that in the investigated residues the X-ray diffraction lines belonging to PbO were not found. This is probably due to the small sizes of crystallites dispersed in the residue.

Before the phase transformation, after a thermal treatment of one hour at 600°C the crystalline phase of the residue consists mainly of γ-Fe_2O_3 (Table 4) and contains small amounts of a mixed oxide, namely $PbFe_4O_7$. The content of this mixed oxide decreases with the time of mixing, which can be explained by taking into account that the generation of oxides with a higher PbO/Fe_2O_3 ratio than that in hexaferrite is favoured by the reduced homogeneity of the precursors.

Table 4 Structural data for the calcination products at 600°C (1 h)

Precursor	Crystallinity/%	a_o/Å	V/V_{ASTM}	d*/Å
P_1/5 min	80	8.3654	1.0051	235
P_2/10 h	87	8.3591	1.0069	243
P_3/20 h	100	8.3602	1.0037	304

*mean crystallite sizes

Thermal treatment performed after the phase transformation (calcination at 800°C for one hour) leads to the formation of the lead hexaferrite $PbFe_{12}O_{19}$ as the main product containing an impurity of α-Fe_2O_3 (Table 5). The values of the lattice parameters are higher than those given by the ASTM 31-686 file. This lattice deformation is probably due to the formation of two mixed oxides with hexagonal lattice, namely $PbFe_4O_7$ (a_o=5.88 Å, c_o=23.02 Å) and $PbFe_{12}O_{19}$ (a_o=11.86 Å, c_o=47.04 Å). A decrease in hexaferrite content with respect to $PbFe_4O_7$ is favoured by higher mixing times of the reactants, which leads to a higher homogeneity of the precursors. The amount of the hexaferrite formed with respect to the amount of α-Fe_2O_3 (Table 8) decreases with the time of mixing. The transformation of γ-Fe_2O_3 to α-Fe_2O_3 is accompanied by a significant decrease in the saturation magnetization.

Table 5 Structural data for the calcination products obtained at 800 and 1000°C

	800°C (1 h)			800°C (8 h)			1000°C (1 h)		
	P_1	P_2	P_3	P_1	P_2	P_3	P_1	P_2	P_3
$PbFe_{12}O_{19}$									
a/Å	5.9003	5.9123	5.8909	5.9108	5.9151	5.9139	5.9490	5.9186	–
c/Å	23.1117	23.140	23.0676	23.1382	23.1294	23.1333	23.1304	23.2231	–
$*V/V_{ASTM}$	1.0088	1.0164	1.0058	1.0157	1.0168	1.0165	1.0180	1.0326	–
d/Å	427	390	363	416	398	362	362	302	
α–Fe_2O_3									
c/Å	5.0405	5.0458	5.0377	5.0395	5.0412	5.0472	5.0472	5.0460	5.0567
a/Å	13.7696	13.7565	13.7919	13.8110	13.8366	13.7823	13.7823	13.8392	13.8982
V/V_{ASTM}	1.0053	1.0053	1.0040	1.0061	1.0086	1.0069	1.0069	1.0107	1.0194
d/Å	308	277	390	362	265	354	354	303	338

*V – means fly volume of the elementary cell.

A longer treatment at the same temperature (800°C, eight hours) leads to the formation of well crystallized lead hexaferrite. The values of the mean size of crystallites are close to those obtained for the same compound after one hour at the same temperature. This result shows that the increase of the calcination time does not affect sample sintering. All the calcination residues contain small amounts of α-Fe_2O_3. The 'cleanest' residue with respect to α-Fe_2O_3 is obtained from the precursor P_2, as shown in Table 6.

Table 6 The phase composition of the calcination products (800 and 1000°C) expressed as the ratio $PbFe_{12}O_{19}/\alpha$-Fe_2O_3 obtained from diffraction data

Thermal treatment	P_1 (5 min)	P_2 (10 h)	P_3 (20 h)
800°C (1 h)	3.70	3.11	0.69
800°C (8 h)	5.33	6.71	1.754
1000°C (1 h)	2.00	1.85	–

A higher temperature of calcination (1000°C, one hour) leads to the generation of α-Fe_2O_3 as well as to a decrease in the crystallite sizes of $PbFe_{12}O_{19}$ and its dispersion in the residue. This phenomenon connected with the precursor's homogeneity (Table 6) may explain the apparently contradictory results obtained by X-ray diffraction and magnetic measurement techniques. So, while the magnetic measurements evidenced the presence of a magnetic phase in all three residues in the X-ray spectra the diffraction lines belonging to lead hexaferrite are identified only in the residues of P_1 and P_2. In other words, $PbFe_{12}O_{19}$ crystallites of very small sizes present in the third residue P_3 are X-ray amorphous. The reasons for such an unexpected behaviour are not yet clear. The values of the lattice parameters for the $PbFe_{12}O_{19}$ in the calcination products of precursors P_1 and P_2 are close to those given in the ASTM 31–686 file.

Table 7 Saturation magnetization of the calcination products

Thermal treatment	P_1 (5 min) σs (emu/g)	P_2 (10 h) σs (emu/g)	P_3 (20 h) σs (emu/g)
600°C (1 h)	8.320	24.520	47.860
800°C (1 h)	linear behaviour, could reach σs	7.830	5.003
800°C (8 h)	8.324	9.933	3.812

The following overall mechanism is proposed for the thermal transformation of the precursors to hexaferrites:

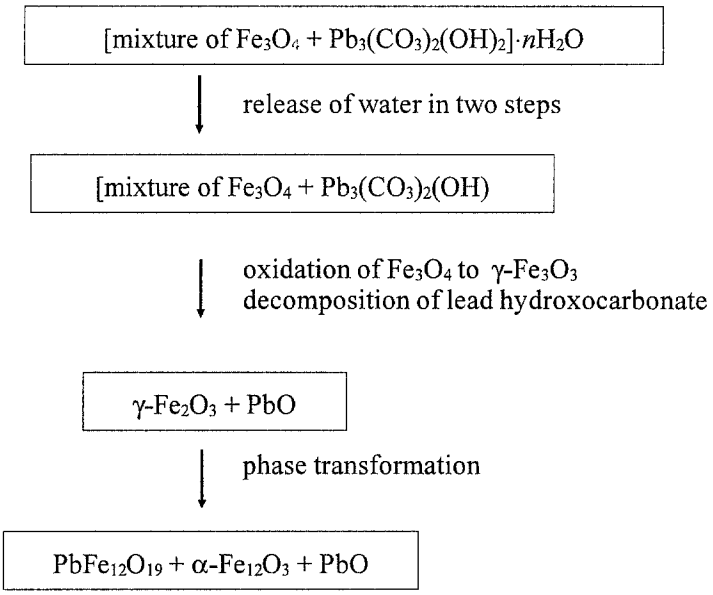

This mechanism describes the changes occurring in the crystalline phases of the original mixture and its decomposition intermediates.

Conclusions

1. A procedure was suggested for the synthesis of some precursors of lead hexaferrite.

2. The properties of the precursors were investigated.

3. The calcination products of the precursors obtained at 600, 800 and 1000°C were analysed and characterized.

4. The investigations revealed that 800°C is the optimum temperature for the preparation of mixed oxides with the properties of lead hexaferrite and with small particles.

References

1 G. Heimke, Z. Angew. Phys. 15 (1963) 271.
2 G. Heimke, Z. Angew. Phys. 71 (1964) 181.
3 K. Hameda and H. Kojima, J. Am. Cream. Soc., 57 (1974) 68.
4 C. D. Mee and J. C. Jashke, J. Appl. Cream. Soc., 53 (1970) 192.
5 K. Hameda, H. Mijaka and H. Kojima, J. Am. Ceram. Soc., 57 (1974) 354.
6 T. Fujiwara, IEEE Trans. Mag., 21 (1985) 1480.
7 S. D Kulkarni, C. E. Desphande, J. J. Shrotri, V. G. Gunjikar and S. K. Data, Thermochim. Acta, 153 (1989) 47.

8 B.T. Shirk and W. R. Buessen, J. Am. Ceram. Soc., 53 (1970) 192.
9 K. Oda, T. Yoshio, K. Oka and F. Kanamaru, J. Mat. Sci. Lett., 3 (1981) 1007.
10 O. Kubo, T. Ioto and M. Kokoyama, IEEE Trans. Mag., 18 (1982) 1122.
11 B. J. J. Zelinski and D. R. Uhlmann, J. Phys. Chem. Solids, 45 (1984) 1069.
12 Xi-Jing Fan and E. Matijevic, J. Am. Ceram. Soc., 71 (1) (1988) 80.
13 T. Tsuchiya, K. Yamashiro and J. D. Mackenzie, J. Ceram. Soc. Jpn. Inter. Ed., 97(93) (1989) 903.
14 J. C. Bernier, Mater Sci. Rng., A-109 (1989) 233.
15 M. Matsumoto, IEEE Trans. J. Mag. Jpn., 6 (1991) 648.
16 C. Surig, K. A. Hempelt and D. Bonnenberg, Appl. Phys. Letters, 63 (1993) 2836.
17 K. Kaneda and H. Kojima, J. Amer. Ceram. Soc., 57 (1974) 354.
18 D. Barb, L. Diamandescu, A. Rusi, D. Tarabasanu, R. Mihaila, M. Mararíu and V. Teodorescu, J. Mater. Sci., 21 (1986) 1118.
19 R. Chandrasekhar, S. W. Charles, K. O'Grady, S. Morup and J. van Wonterghem, Adv. Ceramic Material, 2 (1987) 65.
20 N. G. Error and T. M. Loehr, J. Solid State Chem., 12 (1975) 319.
21 R. Ardiaca, R. Ramos, A. Isalque, J. Rodriguez, X. Obrados, M. Pernet and M. Vallet, IEEE Trans. MAG, MAG-23, 1 (1987) 22.
22 M. Brezeanu, E. Tatu, S. Bocai, O. Brezeanu, E. Segal and L. Patron, Thermochim. Acta, 78 (1984) 351.
23 M. Brezeanu, O. Brezeanu and E. Segal, Thermochim. Acta, 78 (1984) 445.
24 O. Carp, E. Segal, L. Patron, R. Barjega, C. Craiu, N. Stanica and E. Segal, Thermochim. Acta, 78 (1984) 445.
25 O. Carp, E. Segal, M. Brezeanu, L. Patron, R. Barjega and N. Stanica, Thermochim. Acta, 243 (1994) 43.
26 O. Carp and E. Segal, Rev. Roum. Chim., 39 (1994) 1123.
27 H. Klug and L. E. Alexander, 'X-ray Diffraction Procedure' Eds John Wiley & Sons, NY 1962, p. 461.
28 K. Hauffmann and F. Hazel, J. Inorg. Nucl. Chem., 37 (1975) 1139.
29 R. A. Niquist and R. O. Kagel, 'Infrared Spectra of Inorganic Compounds', Academic Press, N.Y. 1976.
30 H. E. Kissinger, J. Rest. Nat. Bur. Stand., 57 (1956) 217.
31 G. Winkler, Z. Angew. Phys., 221 (1966) 282.